Imaging Therapeutic Proteins in Gelatin for Controlled Drug Release

Amy Wagoner Johnson,[1] Nilda Juan Serrano,[2] Abby Whittington Morgan,[2] Russell Jamison,[2] Young Bin Choy,[3] Hyungsoo Choi,[3] Kyekyoon (Kevin) Kim,[3] Francesco DeCarlo[4]*

[1]Department of Mechanical and Industrial Engineering, University of Illinois at Urbana-Champaign, 1206 W. Green St., Urbana, IL, 61801, USA
Email: ajwj@uiuc.edu
[2]Department of Materials Science and Engineering, University of Illinois at Urbana-Champaign, 1304 W. Green St., Urbana, IL, 61801, USA
[3]Department of Electrical and Computer Engineering, University of Illinois at Urbana-Champaign, 1406 W. Green St., Urbana, IL, 61801, USA
[4]Advanced Photon Source, Argonne National Laboratory, 9700 Cass Ave., Argonne, IL, 60439, USA

Summary: Preliminary results from this study show that x-ray microcomputed tomography can be used to image model proteins for bone inducing growth factors. Small quantities (<1 μg protein/mg gelatin) of soybean trypsin inhibitor labeled with either gold nanoparticles or nonradioactive iodine were detected using synchrotron radiation. These results could lead to a new method of measuring the release profile of therapeutic proteins.

Keywords: confocal microscopy; drug delivery systems; protein; tomography; x-ray imaging

Introduction

In response to an event disrupting bone function, such as disease or trauma, proteins are secreted to initiate healing. Disease and other factors can diminish the ability of bone to self-repair. Therefore, augmentation through the use of artificial bone may be required. The addition of therapeutic proteins, or growth factors, to engineered bone constructs is believed to elicit a more natural response at the defect site and to decrease healing time [1]. Drug delivery vehicles must be carefully engineered in order to optimize the dose and dose rate and these parameters must be monitored over time and space. One technique used to measure the pharmacokinetics of growth factors is radioactive labeling [2]. However, this only yields an average value over the sample; it does not provide a 3D description. The radioactivity of the label adds further complications.

 DOI: 10.1002/masy.200550929

Preliminary results from this study demonstrate the feasibility of imaging proteins using x-ray microcomputed tomography (micro-ct) for drug release applications. Soybean trypsin inhibitor (STI), a model protein for the growth factor BMP-2, was labeled with either gold nanoparticles or nonradioactive iodine to provide x-ray absorption contrast and was imaged using micro-ct at the Advanced Photon Source, Argonne National Laboratory. Gelatin microspheres, engineered to produce a controlled release of the growth factor, were loaded with one of the labeled proteins and incorporated into a gelatin sheet. Both the loaded microspheres and the sheet containing the loaded microspheres were imaged and quantities as low as 1 μg protein/mg gelatin were detected. This technique may offer an alternative method to generate a 3D representation of the pharmacokinetics, rapidly, and without radioactive tracers by correlating measured attenuation with label, and therefore, protein concentration. Furthermore, the technique has potential for *in vivo* applications [3,4]. Results will have significant impact on clinical design of bone implants.

Experimental

Preparation of Carrier Matrix. *Gelatin Microspheres.* Gelatin microspheres of isoelectric point (pI) 9.0 were created by a water-in-oil emulsion technique [5]. Briefly, 10 mL of a 10 wt% gelatin solution was added to olive oil to create a water-in-oil suspension. The solution was stirred for 10 min at 40 °C and then cooled to 4°C to precipitate the gelatin microspheres. The microspheres were washed several times with acetone and collected by centrifuge (5000 rpm, 4 °C, 5 min). After allowing the acetone to evaporate overnight, the microspheres were crosslinked using 500 μL gluteraldehyde per 20 mg microspheres, washed with 100 mM glycine (*Sigma*), and freeze-dried. Microspheres made by this method are irregular in shape and can range in size from 20-100 μm.

Gelatin Sheets. Sheets of acidic gelatin were made using the method described by Kang *et al.* [6]. The gelatin solution was crosslinked with gluteraldehyde overnight at 4°C. The gels were cut to size and the crosslinking was terminated 8-10 hr later with 100 mM glycine for 1hr at 37°C. After washing in distilled water to remove the residual glutaraldehyde and glycine, the sheets were suspended in a small volume of water, frozen overnight at -80°C, and then lyophilized for 72 hours.

Protein Labeling. The model protein, STI (*US Biological*), was used in lieu of the growth factor of interest, BMP-2, because of the similar molecular weight and number of amine

groups, and the significantly lower cost, as are shown in Table I. The number of aromatic groups did not match as well. The amine groups provide potential sites for gold conjugation by 2-Iminothiolane•HCl, (Traut's reagent, *Pierce*), which reacts with primary amine groups (-NH_2) to introduce sulfhydryl groups (-SH), while maintaining charge properties similar to the original amino group [7,8]. Once added, sulfhydryl will bind strongly to the surface of the gold [9,10]. The aromatic groups provide sites for iodination of the protein [11]. In particular, chloramine-T (*Sigma*) has strong oxidizing properties that readily lead to the formation of the required electrophilic halogen species that result in iodine incorporation into target molecules [11]. Four conditions were prepared and studied, all of which contained Au- or I-labeled STI incorporated into gelatin microspheres. The cases considered were: (1) microspheres in gelatin sheets with Au-labeled STI (μ-sheet-Au-STI), (2) microspheres in gelatin sheets with I-labeled STI (μ-sheet-I-STI), (3) microspheres with Au-labeled STI (μ-Au-STI), and (4) microspheres with I-labeled STI (μ-I-STI).

Table I. Comparison of BMP-2 to model protein, Soybean Trypsin Inhibitor (STI).

Protein	MW (kD)	pI	*(-NH2)/protein*	Aromatic group/protein	Price/μg ($)
BMP-2	25	8.5	19	21	20
STI	21.5	4.6	20	6	.001

Gold Conjugation. A weight of 2.5 mg of the unlabeled STI was dissolved in a non-amine buffer with pH 8.0 (50mM triethanolamine, 0.15M NaCl, 1 mM EDTA). A 5-fold molar excess of Traut's reagent (40 μL) was subsequently added to the protein in solution and incubated for 1 hour at room temperature. The reagent excess was separated from the thiolated protein using a desalting column equilibrated with 3 mM EDTA/phosphate buffer (PBS), and the protein concentration was determined using the BCA Protein Assay (*Pierce*) and by measuring the absorbance at 562nm with a spectrophotometer.

The pH of the gold colloid (*Ted Pella, Inc.*) was adjusted to the isoelectric point of the protein to maximize the binding and the stability of the complex [12], using 0.2 M K_2CO_3 and 1M H_3PO_4. Following the ratio suggested by the manufacturer (1 mL colloidal gold per 10 μg protein), 35 mL of colloidal gold was added to 1 mL of the thiolated protein and the solution was incubated overnight at 4°C. The gold-protein complex was centrifuged at 12,000 rpm for 20 minutes and the supernatant discarded. The gold-labeled protein was then diluted to 1 mL PBS, pH 7.4, and the concentration measured as described above.

Iodination. First, the protein (1 mg) was dissolved in 1 mL of PBS. A volume of 100 μL of the protein/PBS solution was mixed with 50 μL of 5M NaI solution. The reaction was initiated using 1 mL of 0.9 mM Chloramine-T in PBS and was stopped using 1 mL of freshly prepared 21 mM sodium metabisulfite in double distilled water. The iodinated protein solution was poured through an ion exchange column made of Dowex Anion Exchange Resin 1x8-400(Cl) (*Fisher*) in a 2.5 mL syringe equilibrated with PBS, and then incubated overnight at 4°C [13,14]. The labeled protein concentration was measured as described above.

A volume of 120 μL of each labeled proteins was added to 12 mg of freeze-dried gelatin microspheres. After two hours at room temperature, the microspheres in solution were diluted in 210 μL of PBS. Samples were taken from the two microsphere solutions and used as the μ-Au-STI and μ-I-STI samples. The final concentration of the labeled protein in the microspheres was approximately 0.75 μg protein/mg gelatin microspheres. The remainder of each of the two microsphere solutions was used to make the μ-sheet-Au-STI and μ-sheet-I-STI samples by injecting 80 μL and 100 μL of the solution, respectively, into 5 mm diameter gelatin sheets using a syringe.

Microcomputed Tomography. Micro-CT experiments were conducted at beamline 2-BM, of the Advanced Photon Source, Argonne National Laboratory using synchrotron radiation. Full details of the experimental set-up can be found in Wang *et al.* [15]. Prior to imaging, all samples were deposited on the sample mount and dried using acetone. Imaging wet specimens was not possible due to sample movement induced by beam heating. The incident monochromatic energy was 19.1 keV and the data acquisition time for a 1024x1024 single projection with 720 total projections was approximately 10 minutes. The field of view was 2.5 mm and, under these conditions, the spatial resolution was 2.4 μm/voxel. The gelatin sheets were cut to fit completely within the field of view in order to ensure clean reconstructed images. The microspheres were piled into a column of approximately 1 mm in diameter for imaging. The data collected were reconstructed as a series of cross-sectional images with the measured linear attenuation associated with each voxel element. Control samples, including unlabeled STI incorporated into gelatin microspheres (μ-STI), and gelatin sheet without STI (sheet), were also imaged for comparison.

Data Sampling. The number of voxels for each attenuation value was plotted in the form of a histogram for the entire sample. Because of the minute quantities of protein (1 μg protein/mg microsphere) compared to the volume of background and gelatin in the data set, the histogram did not reveal any useful information. Therefore, specific regions were sampled locally and histograms made in order to distinguish the regions containing the gold or iodine from the rest of the specimen. For data rendering, we used Amira™ from Indeed - Visual Concepts GmbH. Locally sampled regions for the sheets and the microspheres included the background, two types of artifacts (line and ring), control gelatin sheets with and without background (i.e. at the center or on the edge of the sheet), and regions believed to contain the Au- or I-labeled protein. For the analysis of the sheet and the microspheres, four representative volumes containing 3 - 5 x 10^4 voxels each, and 15 volumes containing 3 x 10^2 voxels each were sampled, respectively, from different cross sections of the same specimen. In order to obtain a representative region of the microspheres containing the labeled protein without a large volume of background, much smaller volumes were sampled.

Confocal Microscopy. Confocal microscopy was used to image the Au-labeled microspheres for comparison to micro-ct results. Samples were mounted in glycerol/PBS (9:1, refractive index = 1.45) and imaged using a Leica SP2 Confocal and Multiphoton microscope equipped with a Krypton Argon Laser. Data was collected from two channels simultaneously; one channel recorded the autofluorescence from the gelatin, the other the reflected light from the gold. Image volumes were assembled from a vertical series of images with focus control provided by a precision microstepping motor. The iodinated protein will not fluoresce or reflect light and therefore could not be imaged in this manner.

Results

Representative grey scale images of the μ-sheet-Au-STI and μ-Au-STI are shown in Figures 1a and 1b, respectively. This paper focuses on the Au-labeled protein; results were similar for the gold and iodine data. Localized bright spots are visible in both figures. The high contrast regions represent regions of higher attenuation and are thus indicative of the presence of Au (or I). Representative regions are enlarged in the insets (see black arrow and inset). In Figure 1b, the bright spots are concentrated near the outside of the microspheres, while in the sheet they are more concentrated in the vicinity of the tears created by the syringe (see black arrow). The concentric rings in Figure 1a,

shown by the white arrow, are a common artifact and are unrelated to the sample. The microspheres are small relative to the rings in Figure 1b and are therefore the artifact is less prominent. Another type of artifact, a line artifact, is smaller than the ring artifact, but is usually seen near sharp corners extending beyond the sample into the background. The images shown do not contain especially prominent line artifacts.

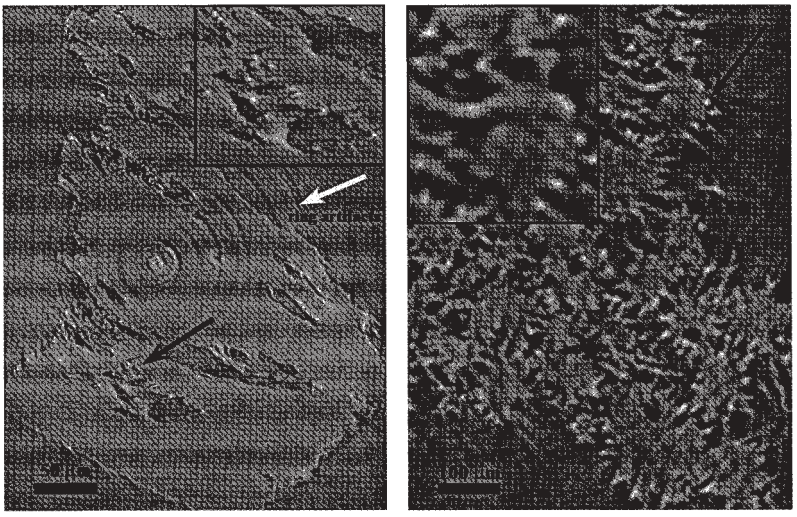

Figure 1. Cross-sectional micro-ct images of (left) a gelatin sheet injected with microspheres loaded with the Au-labeled model protein, soybean trypsin inhibitor (STI), and (right) microspheres containing Au-labeled STI. Insets show enlargements of the regions indicated by the black arrow. Ring artifacts are shown in (a) near the white arrow. Note the concentrrated bright spots in each image, indicative of a higher attenuation, and therefore the presence of the gold nanoparticles. Iodinated samples showed similar results.

Figure 2 shows attenuation data from the one of the four representative sample volumes from the μ-sheet-Au-STI and the μ-sheet-I-STI specimens in the form of a histogram. Using the micro-ct images alone is not sufficient for interpreting the high contrast regions as regions containing Au or I; some artifacts also cause high contrast, which could be mistaken for the labels. These data clearly show that the samples containing Au- and I-labeled STI can be distinguished from other samples; the sample volumes show distinctly different peaks. The largest distinction is that these peaks are asymmetric, with long tails extending to high attenuation values. This is a strong indication that the microgram quantities of labeled protein can be detected in the gelatin sheets, and can be distinguished from background and other artifacts. The background peak, both with and without the

control gelatin sample, is undisputably distinguishable from all of the other sample volumes. The peaks from the ring and line artifacts are near zero and are both symmetric.

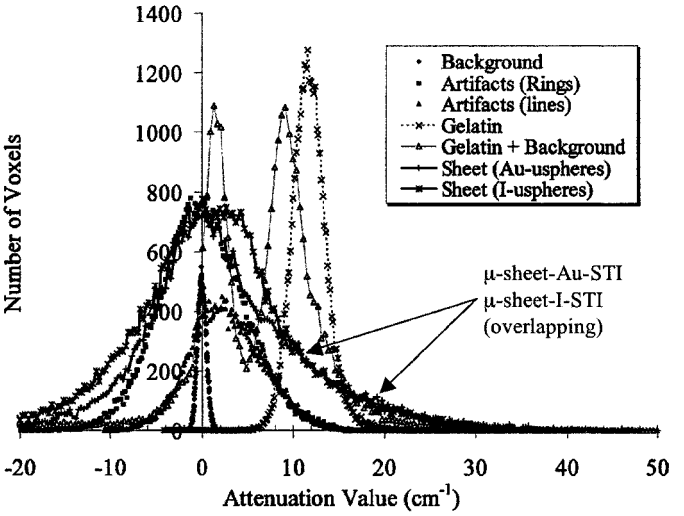

Figure 2. Micro-ct data for gelatin sheets containing Au- or I-labeled protein in gelatin microspheres in the form of a histogram. These data were obtained by locally sampling regions in cross-sectional images. The data demonstrate that the regions containing the labeled protein can be distinguished from artifacts and control gelatin samples by their asymmetric shape and higher number of voxels at the highest measured attenuation.

The sample volume of the control gelatin shows a very distinct and narrow peak centered around 11 cm^{-1}. In the volume containing background and gelatin, the individual peaks are clearly distinguishable. The regions of the specimen containing the labeled protein loaded into the microspheres and then injected into the gelatin sheet contain only small amounts of labeled protein, and significant amounts of gelatin. Therefore large numbers of voxels with high attenuation were not expected. In comparing the efficacy of the gold versus the iodine labels, the data do not suggest that one is better than the other.

The attenuation data from sample volumes of the μ-Au-STI, μ-I-STI, and μ-STI samples are shown in Figure 3. A moving average over 75 data points is shown using the solid curves. The data from the μ-STI have a relatively symmetric peak, centered around 25 cm^{-1}. Both the μ-Au-STI and the μ-I-STI have relatively asymmetric peaks, with more voxels with higher attenuation values for the same sampled volume. This data also

strongly suggests that microgram quantities of Au- or I-labeled proteins can be detected in the gelatin microspheres using micro-ct.

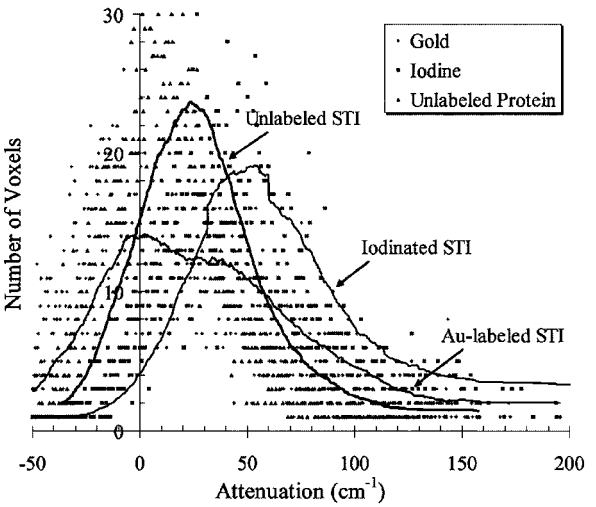

Figure 3. Micro-ct data for gelatin microspheres containing Au- or I-labeled protein in the form of a histogram. These data were obtained by sampling small volumes of select regions in cross-sectional images. The bright spots near the outside of the microspheres are associated with the labeled protein.

Confocal microscopy was used to support micro-ct results for the μ-Au-STI samples and representative images are shown in Figures 4. Gelatin microspheres without STI and microspheres with unlabeled STI were used as controls. The top row of images in Figure 4 shows composite 3D images from both the autofluorescent microsphere and the reflected light from the gold nanoparticles. Autofluorescence is observed in the microspheres due to the gluteraldehyde crosslinking. The bottom row of images shows only the reflected light. Clearly, the sample containing the gold reflects more light than the control samples and the distribution of the additional reflected light is consistent with the results obtained from micro-ct; the gold is concentrated near the outer surface of the microsphere and in the pockets or folds of the irregular surface of the sphere. Some reflected light is also present in the control samples, and this is caused by the index of refraction mismatch between the gelatin/protein combination and the mounting medium. A mounting medium with a better match is being investigated.

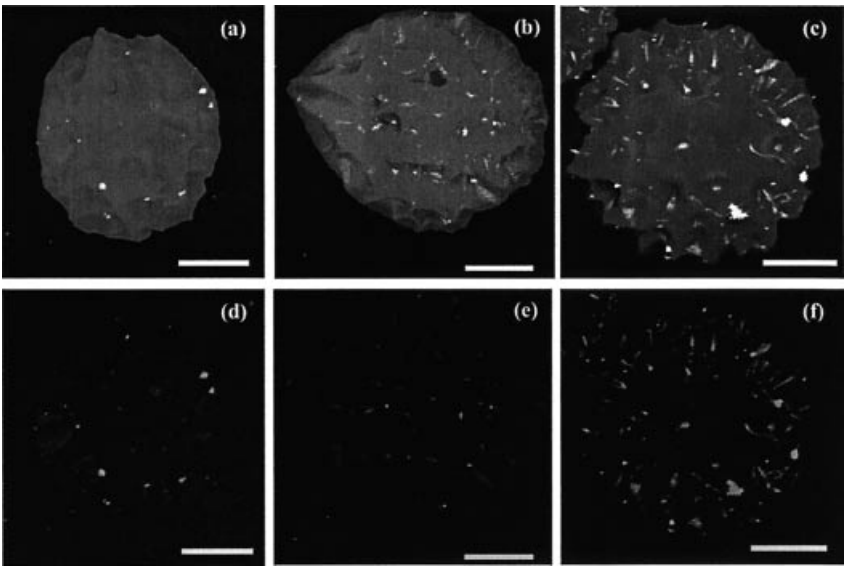

Figure 4. Representative confocal images of the gelatin microspheres. Images (a-c) are composite images made from the fluorescent and reflected light. Images (d-f) are the show the reflected light only. (a) An empty microsphere, (b) a microsphere containing unlabeled protein, and (c) a microsphere containing the Au-labeled model protein, soybean trypsin inhibitor. Scale bar is 40 microns.

Summary and Conclusions

The study demonstrates the use of micro-ct for detecting Au- and I-labeled therapeutic proteins for controlled drug release applications. Micro-ct has advantages over alternative techniques because it is non-destructive, little sample preparation is required, and millimeter-sized samples can be imaged with resolution less than 3 μm. The advantage of using gold nanoparticles as a drug label is that the particles are nontoxic, nonradioactive, and are less disruptive to the activity of the protein [12,16] than is the iodine (radioactive or nonradioactive).

The results from this study specifically show that microgram quantities of Au- and I-labeled soybean trypsin inhibitor, a model protein for the bone inducing growth factor BMP-2, per milligram of gelatin can be detected using synchrotron micro-ct. There is no apparent difference in measured attenuation for the gold versus the iodine label, which we rationalize in the following way. In the case of nano-sized particles, a single particle attaches to each protein molecule [17], while a total of six iodine atoms can theoretically

attach [18,19]. Even though the relative linear attenuation of gold relative to iodine is high (10:1), we speculate that multiple sites per protein molecule were occupied by iodine, while the total protein concentration in Au- and I-labeled samples was equal. As a result, samples containing iodine showed similar attenuation values as those containing gold. The advantage of using the gold is that it is less likely to denature the protein and can be detected using other methods, such as with confocal or transmission electron microscopy, in order to confirm results. Here, confocal microscopy showed results consistent with those from the micro-ct experiments.

Micro-ct is a non-invasive technique and there is significant potential for using this method of drug detection *in vivo*. The latter is especially true when considering drugs used in higher concentrations, for example in milligram rather than microgram quantities [3,4], and as the resolution of computed tomography improves with technological advances.

Acknowledgements

The gelatin used was kindly donated by Nitta Gelatin Co. (Japan). The authors acknowledge support from the Gates Millenium Scholarship program (NJS). The authors thank the following people from the University of Illinois for contributing their time and expertise: Abigail Wojtowicz, Professor Dan Pack, and Dr. Karl Garsha and Daniel Webber of the Beckman Institute. Use of the Advanced Photon Source was supported by the U.S. Department of Energy, Office of Science, Office of Basic Energy Sciences, under Contract No. W-31-109-ENG-38.

[1] M. Joyce, S. Jingushi , M. Bolander, *Ortho Clin N Amer,* **1990**, *21*, 199.
[2] Y.Yu , J.-L.Yang, P. J. Champman-Sheath, W. R. Walsh, *J Biomed Mater Res,* **2002**, *60*, 392.
[3] A. Szymanski-Exner, N. T. Stowe, K. Salem, R. Lazebnik, J. R. Haaga, D. L. Wilson, J. Gao. Noninvasive Monitoring of Local Drug Release Using X-ray Computed Tomography: Optimization and In Vitro/In Vivo Validation, *J Pharm Sci*, **2003**, *92 (2)*, 289.
[4] A. Szymanski-Exner, N. T. Stowe, R. S. Lazebnik, K. Salem, D. L. Wilson, J. R. Haaga, J. Gao, Noninvasive monitoring of local drug release in a rabbit radiofrequency (RF) ablation model using X-ray computed tomography, *J Control Release,* **2002**, *83*, 415.
[5] Y. Tabata, Y. Ikada, K. Morimoto, H. Katsumata, T. Yabuta, K. Iwanaga, M. Kakemi, Surfactant free preparation of biodegradable hydrogel microspheres for protein release, *J Bioact Compat Pol,* **1999**, *14,* 371.
[6] H. W. Kang, Y. Tabata, Y. Ikada, Fabrication of porous gelatin scaffolds for tissue engineering, *Biomaterias,* **1999**, *20*, 1339.
[7] R. Traut, Methyl 4-mercaptobutyrimidate as a cleavable cross-linking reagent and its application to the Escherchia coli, *Biochem J* **1973**, *12*, 3266.
[8] Jue, Lambert, Pierce, R. Traut R, Addition of sulfhydryl groups to Escherchia coli ribosomes by protein modification with 2-iminothiolane (methyl 4 mercaptobutyrimidate). *Biochem*, ***1978***, *17*, 5399.
[9] A. Kudelski, Structures of monolayers formed from different HS-(CH2)2-X thiols on gold, silver and copper: comparative studies by surface-enhanced Raman scattering, *J Raman Spectrosc*, **2003**, *34*, 853.
[10] K. Prime, G. Whitesides, Self-assembled organic monolayers: model systems for studying adsorption of protein at surfaces, *Science*, **1991**, *252*, 1164.
[11] D. S. Wilbur, Radiohalogenation of Proteins: An Overview of Radionuclides, Labeling Methods and Reagents for Conjugate Labeling, *Bioconjugate Chem*, **1992**, *3*, 433.
[12] Colloidal Gold Principles, Methods and Applications, M. A. Hyat, ed., Academic Press, San Diego Press, 1989, 38.
[13] D. S. Wilbur, S. W. Hadley, M. D. Hylarides, P. G. Abrams, P. A. Beaumier, A. C. Morgan, J. M. Reno, A. R. Fritzberg, Development of a stable radioiodinating reagent to label monoclonal antibodies for radiotherapy of cancer, *J Nucl Med*, **1989**, *30,* 216.
[14] A. E. Bolton, W. M. Hunter, The labeling of proteins to high specific radioactivities by conjugation to a 125I- containing acylating agent, *Biochem J*, **1973**, *133*, 529.
[15] Y. Wang, F. D. Carlo, D. Mancini, I. McNulty, B.Tieman, J. Bresnahan, I. Foster, J. Insley, P. Lane, G. V. Laszewski, C. Kesselman, M. –H. Su, M. Thiebaux, High-throughput x-ray microtomography system at the Advanced Photon Source, *Rev Sci Intstrum*, **2001,** *72*, 2062.
[16] S. L. Goodman, G. M. Hodges, D. C. Livingston, A review of the colloidal gold marker system, *Scan Electron Microsc,* **1980**, *11*, 133.
[17] J. E. Beesley, Colloidal gold: A new perspective for cytochemical marking, J. E. Beesley, ed., Microscopy Handbooks. New York: Oxford University Press, 1989.
[18] National Center for Biotechnology Information (NCBI). U.S. National Library of Medicine, Bethesda, MD, January 19, 2005 (Accessed March 6, 2004) <http://www.ncbi.nlm.nih.gov/>.
[19] SDSC Biology WorkBench. San Diego Supercomputer Center- University of California San Diego, July 10, 2003 (Accessed March 6, 2004), <http://workbench.sdsc.edu/>.